

# A COMPARATIVE STUDY OF MODE I FATIGUE CRACK PROPAGATION IN FOAM CORES FOR SANDWICH STRUCTURES BY USING DIFFERENT TEST SPECIMENS

Andrey Shipsha, Magnus Burman, Dan Zenkert

*Department of Aeronautics  
Division of Lightweight Structures  
Royal Institute of Technology  
100 44, Stockholm, Sweden*

**SUMMARY:** This paper summarizes results on mode I fatigue crack growth (FCG) in foam core materials for sandwich structures. The studies deal with characterization of the FCG in the face/core interface in sandwich beams and in the virgin foam core. The core material properties, test specimens and experimental procedures are briefly described. Stress intensity factors  $\Delta K$  in the vicinity of the crack tips are computed using the finite element method. The obtained FCG rates  $da/dN$  in the investigated specimen configurations are combined in standard  $da/dN$  versus  $\Delta K$  curves. Fatigue behaviour of the cellular foams appear to conform to the classical Paris' law. The influence of face/core interface on mode I FCG rates is discussed in comparison to the FCG rates in the virgin core. The FCG rates in the face/core interface in sandwich beams are verified using the Tilted Debond Sandwich (TDS) specimen.

**KEYWORDS:** fatigue, crack growth, fatigue threshold, foam core, sandwich structures

## INTRODUCTION

A development and design of modern construction, utilizing structural sandwich elements, require an extensive knowledge of the mechanical properties of sandwich components, in particular, the core material, which is the weakest and most critical constitutive. Cellular foams are commonly used as a core material in sandwich structures. They simultaneously provide reasonably good mechanical properties and the low density. Basic mechanical and physical properties of foams have been thoroughly studied by Gibson and Ashby [1]. However, such phenomena as fatigue crack nucleation and propagation, the effect of foam microstructure on the growth of fatigue cracks have so far received little attention and still have to be studied.

Static tests on mode I crack propagation in rigid PVC cellular foams were conducted by Zenkert and Bäcklund [2]. They also performed mode II and mixed-mode fracture tests [3] and showed that linear elastic fracture mechanics (LEFM) can be used to characterize fracture in the foam cores. A dependence between cell size and fracture toughness was found for PUR foams by McIntyre and Anderton [4] and for PVC foams by Zenkert and Bäcklund [2].

Fatigue crack propagation under mode I and mode II in PVC and PMI foam core sandwich beams with interfacial defects have been studied by Shipsha *et al.* [5] using the Cracked Sandwich Beam (CSB) and the Double Cantilever Beam (DCB) specimens. The fatigue crack was found to propagate in the core material at a distance of 1-2 cells underneath the face/core interface. The FCG rates and fatigue threshold values  $\Delta K_{th}$  for an interfacial crack subjected to mode I and mode II propagation were determined.

Noury *et al.* [6] investigated fatigue crack growth under combined mode I and mode II loading using the Compact-Tension-Shear (CTS) specimen in rigid PVC cellular foams. Their study also showed that LEFM provides a reasonable description of the considered material. The crack growth regime was accurately modeled by the Paris' law. Later, Shipsha *et al.* [7] conducted the experimental study on mode I fatigue crack propagation in rigid PVC and PMI foam cores using a slightly modified version of the standard Compact Tension (CT) specimen. Values of stress intensity threshold  $\Delta K_{th}$  were derived and the effect of various  $R$ -values on FCG rates was investigated.

The present study summarizes and compares results on mode I fatigue crack propagation in PVC and PMI cores, obtained by the authors in related studies [5,7]. These two studies deal with characterization of the FCG in the face/core interface (DCB specimen) and in the virgin foam (CT specimen). The fatigue data from different tests are combined and plotted in one  $da/dN$  versus  $\Delta K$  graph which provides an illustrative comparison of the results. The influence of face/core interface on mode I FCG rates is examined in comparison to the FCG rates in the virgin core (CT specimen). This paper also verifies the results from the DCB tests using the Tilted Debond Sandwich (TDS) specimen, initially introduced by Li and Carlsson [8].

## EXPERIMENTAL PROCEDURE

### Core material properties

Two core materials, used by the authors in related investigations, were Divinycell<sup>®</sup> H100 and Rohacell<sup>®</sup> WF51, where the number indicates the nominal density in  $\text{kg/m}^3$ . Both materials are cross-linked expanded rigid cellular foams with a closed cell structure. H100 and WF51 have comparable mechanical properties, which are summarized in Table 1, though the WF51 core is more brittle.

*Table 1: Basic mechanical properties of the H100 and WF51 foams used in this investigation, given by the manufacturers [9,10].*

Core Material	Density ( $\text{kg/m}^3$ )	Tensile Modulus (MPa)	Tensile Strength (MPa)	Shear Modulus (MPa)	Shear Strength (MPa)	Cell Size (mm)
H100	100	105	3.1	40	1.4	0.35-0.45
WF51	52	75	1.6	19	0.8	0.50-0.70

## Test specimens

### *Double Cantilever Beam (DCB) specimen*

A modified Double Cantilever Beam (DCB) specimen, illustrated in Fig. 1, was used in the study [5] to investigate the mode I crack propagation in the face/core interface. The specimen was clamped to the rigid foundation. Load was applied via the hinge attached to the end of the specimen to prevent the bending moment deformation of the face. Dimensions of DCB specimen were chosen to satisfy LEFM conditions in the vicinity of the fatigue crack tip.

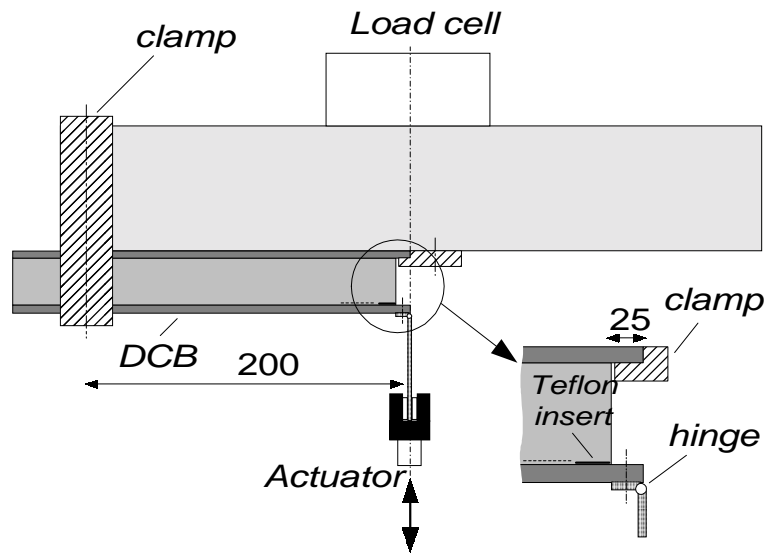


Fig. 1: DCB specimen and test set up. Dimensions are in [mm].

The DCB specimens with a 25 mm core and 3.2 mm laminate faces were manufactured using a hand lay-up technique. The laminates were four layers of E-glass/polyester. To simulate an interfacial debond in the face/core interface, a 125  $\mu\text{m}$  Teflon film was placed between the core and the face. The length of the initial debond was 50 mm in all DCB specimens. The total dimensions of the DCB specimen were 300 $\times$ 31.4 $\times$ 25 mm.

### *Tilted Debond Sandwich (TDS) specimen*

A Tilted Debond Sandwich (TDS) specimen is basically the DCB specimen clamped to the rigid foundation with an arbitrary tilt angle  $\theta$  to the horizontal plane. It was experimentally found in [8] that the imposed tilt angle  $\theta=10^\circ$  for initial crack length of 50 mm produces a component of negative shear at the crack tip and suppresses the interfacial crack kinking at the initial stage of the test, providing the debonding along the face/core interface.

### *Compact tension (CT) specimen*

A modified compact tension (CT) specimen with slightly larger dimensions than the standard CT specimen was used to study the mode I FCG rates in a virgin core [7]. The geometry of the CT specimen is schematically shown in Fig. 2. The dimensions of CT specimen were appropriately chosen to comply with required LEFM conditions in the vicinity of the crack tip, as specified in ASTM standard E647-95a [11]. The thickness of the CT specimen was equal to the core block thickness of 50 mm. Total specimen dimensions were 400 $\times$ 270 $\times$ 50 mm.

In order to avoid scatter caused by light anisotropy the principal directions of all CT specimens were aligned with respect to the principal directions of the core block. The notch simulating an initial crack with  $a/W = 0.4$  was cut out using a thin band saw of 0.8 mm thickness. The sharp crack tip with a length of 1-2 mm was made with a razor blade. None of the specimens were fatigue pre-cracked. The CT specimens were pin-loaded by steel clevises attached to the specimen through the steel tube inserts, as shown in Fig. 2.

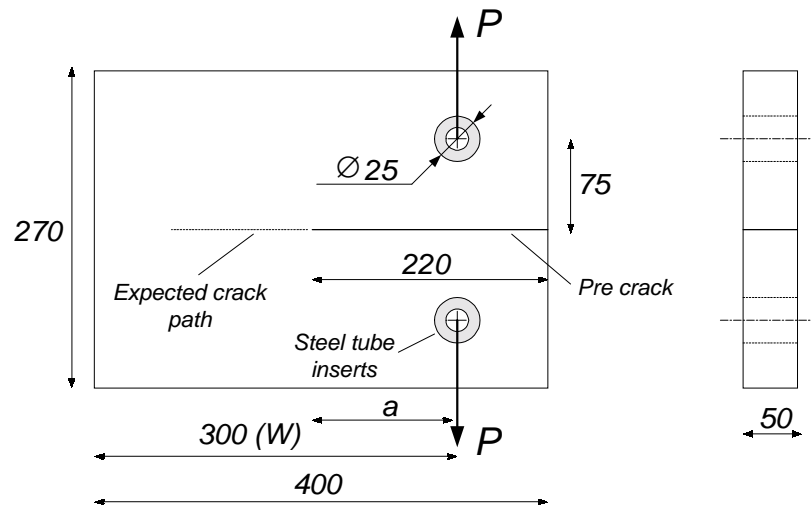


Fig. 2: Compact tension specimen geometry. Dimensions are in [mm].

### Test Set Up

In order to designate the appropriate load levels for fatigue testing, series of static experiments for each material and specimen configuration were performed to determine a static fracture load. The maximum cyclic load,  $P_{\max}$  was chosen to be 60% of the static fracture load. The fatigue testing was conducted in a load control manner with a frequency of 2 Hz. A sinusoidal cyclic load with the load ratio  $R=0.1$  was applied. As the fatigue crack started to grow, its length was measured by means of an optical travelling microscope with magnification of  $\times 10$ . A greater optical magnification is unnecessary because of the difficulty to define the exact position of the fatigue crack tip in a such coarse structure as a cellular foam. The straightness of the crack front through the specimen thickness was verified by spraying a pressurized paint between the crack flanges, close to the crack tip. Then the specimen was broken to check the geometry of the crack front which appeared to be reasonably straight. Therefore, the crack length was measured only on the front surface of the specimen. Fatigue tests were performed under constant load-amplitude which gives rise to  $\Delta K$  values with a crack extension. The FCG rates above  $10^{-6}$  mm/cycle can be achieved by using this technique. When the near-threshold FCG rates below  $10^{-6}$  mm/cycle are sought, a manual load-shedding technique [11,12] was applied resulting in decreasing  $\Delta K$  values with a crack growth. All experiments were performed by using a 10 kN Schenk PSA-10 servo hydraulic testing machine.

### Crack growth data reduction

A secant or a linear differentiation technique, thoroughly described in ASTM E647-95a [11], was employed for data reduction of measured FCG rates in DCB and CT specimens. This method simply computes the slope of the straight line connecting two adjacent data points on the crack length  $a$  versus number of cycles  $N$  curve:

$$\left( \frac{da}{dN} \right)_{\bar{a}} = \frac{a_{i+1} - a_i}{N_{i+1} - N_i} \quad (1)$$

$$\bar{a} = \frac{a_{i+1} + a_i}{2} \quad (2)$$

where the computed crack growth rate  $da/dN$  is an average rate over the  $(a_{i+1}-a_i)$  crack increment. This average rate is related to the average crack length  $\bar{a}$  over the considered crack increment, which is then used to compute stress intensity factors  $\Delta K$ .

### STRESS INTENSITY FACTOR CALCULATIONS

Stress intensity factors for the DCB and the CT test specimens were computed using the finite element (FE) method. Numerical analyses of 2-D linear elastic FE models with implemented eight-node quadratic membrane elements have been performed by using the FE code ANSYS. A static unit load of 1 N/m and boundary conditions relevant to the real test set up were applied. The core material was treated as isotropic and LEFM conditions were assumed. A singular behaviour in the vicinity of the crack tip was modeled by moving mid-side nodes of the surrounding elements to the quarter point locations as shown in Fig. 3. Stress intensity factors were determined by using the displacement extrapolation method. Stress intensity factors were found to be linearly dependent on the crack length.

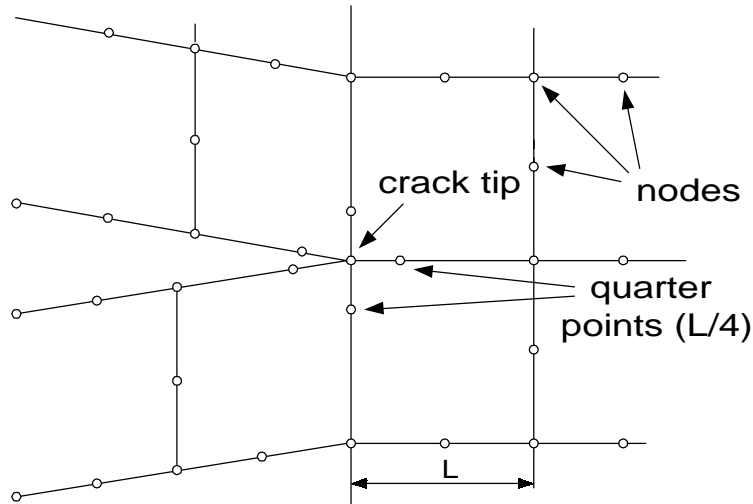


*Fig. 3: Modelling of stress singularity in the crack tip.*

To validate the accuracy of the FE calculations of stress intensity factors for the DCB and the modified CT specimens, the standard CT specimen [11] was modeled in a similar way in the work [7]. The numerically computed stress intensity factors for the standard CT specimen were in a very good agreement with the relevant results derived by using a closed form analytical solution, which is given in [11]. In case of the DCB specimen, the crack propagation path was modeled along the face/core interface and two cells down in the core material, as observed in the tests [5]. Thus, the crack was considered to propagate in a homogeneous, isotropic single medium which significantly simplifies the fracture analysis.

## TEST RESULTS AND DISCUSSION

### Fracture toughness

Series of three to four DCB and CT specimens were tested in static to determine the average fracture loads. Fracture toughness values were obtained by recalculating the stress intensity factors, computed in the FE analyses for the unit load of 1 N/m, in terms of the real fracture loads. Table 2 provides a comparison of fracture toughness values obtained for the DCB and the CT specimens. As can be seen, the values of fracture toughness are in a good agreement for the H100 core material. However, the fracture toughness for the WF51 core material obtained from the DCB test was significantly higher in comparison to the CT specimen results. At the same time, fracture toughness values for the WF51 core, obtained in CT specimen testing, appeared to be in a good correlation with the results in [13]. Therefore, new tests of the DCB specimens with the WF51 core were conducted in this study to verify the fracture toughness values.

*Table 2: Fracture toughness and threshold values of stress intensity factors for DCB and CT specimens.*

Test configurations		Values of $K_{Ic}$ ( $\text{MPa}\sqrt{\text{m}}$ )	Values of $\Delta K_{th}$ ( $\text{MPa}\sqrt{\text{m}}$ )
DCB/TDS specimen	H100	0.210	0.040
	WF51	0.11/0.071*	0.023
CT specimen	H100	0.220	0.035
	WF51	0.072	0.017

\* old value/new value

### *New DCB testing*

In new DCB specimens the initial crack was made by a thin razor as a 50 mm sharp notch between the core and the face, just below the interface. The new DCB specimen dimensions and the test set up were the same as shown in Fig. 2. The obtained static fracture loads for the new DCB specimens were significantly lower in comparison to the previous results in [5].

However, a careful observation of the crack paths in the DCB specimens after static tests revealed that, in case of the WF51 core, the crack initially tends to kink into the core at a certain angle over a length of 4-5 mm and then returns to the face/core interface propagating at the distance of 1-2 cells down along the interface. Li and Carlsson [8] showed that in this case, the assumption of the pure mode I crack is not valid and the mixed-mode stress fields with positive shear stresses force the crack to kink into the core at the initial stage of the test.

### *TDS specimen testing*

To overcome this problem and to verify the fracture toughness values for the DCB specimens with WF51 core, the TDS specimen approach [8] was used in this study. The DCB specimen was bolted to the rigid foundation with the tilt angle  $\theta=10^\circ$  to suppress the crack kinking [8]. No crack kinking into the core was occurred in the new DCB specimens when the TDS approach is used. The fracture toughness values for the DCB and the TDS specimens were found to be identical, in spite of the crack kinking in the DCB specimens. Corrected values of fracture toughness for the WF51 core obtained in DCB/TDS specimens appeared to be in a

good agreement with the results from the CT tests with the WF51 core and they are also given in the Table 2.

The comparison of the results revealed an indication that fracture toughness values, obtained for both core materials in the DCB specimens are lower than relevant values in the CT specimens. Similar behaviour was noticed by Li and Carlsson [8] and believed to be due to the influence of the stiff face and the interface region. However, this hypothesis is the subject for further investigation.

### **Fatigue testing**

Fatigue crack growth data, at least for the stage of stable crack growth, are usually analysed by using the Paris' relationship, which gives a straight line when the experimentally determined FCG rates,  $da/dN$ , are plotted against the amplitude of the stress intensity factor in the vicinity of the fatigue crack,  $\Delta K$ , on a double logarithmic scale:

$$\frac{da}{dN} = C\Delta K^m \quad (3)$$

where  $m$  is the slope of the curve and  $C$  is the point where an extension of the curve will intersect with  $\Delta K=1 \text{ MPa}\sqrt{\text{m}}$ , and  $\Delta K=K_{\max}(1-R)$  is the amplitude of stress intensity experienced by the crack tip in each load cycle.

#### *General considerations*

In previously conducted studies [5,7] the fatigue testing was performed under a constant loading amplitude,  $K$ -increasing technique and under a manual shedding of load amplitude,  $K$ -decreasing technique. The low and intermediate FCG rates obtained by using these testing techniques were in agreement with each other lying on a straight line for the H100 and the WF51 core materials, when plotted in the one  $da/dN$  versus  $\Delta K$  graph. Thus, the Paris' law (Eqn 3) could be used to analyze the fatigue properties of considered foam cores. Even though, several test specimens for each core were tested under nominally identical conditions, the experimental results revealed a moderate scatter. Apparently this is predictable for such type of material as a cellular foam, where the crack propagation is influenced by the foam microstructure. On a microscale level, the process of the fatigue crack extension is rather discrete than continuous since the crack grows through the cellular structure, where only the cell walls can resist the crack propagation.

#### *Comparison of the fatigue data from the DCB and the CT tests*

Fig. 4 presents the comparative plots from the DCB and the CT specimen tests for the H100 and the WF51 cores. All presented results were obtained at load ratio  $R=0.1$  and the maximum load level of 60% of the static fracture load. Various dots in the plots illustrate different test specimens. Straight lines in the plots represent power function curve fits to the experimental data, which were found by using a least square method. Equations for the curve fits, derived and presented in the Fig. 4(a,b), characterize the material properties in terms of the Paris' law.

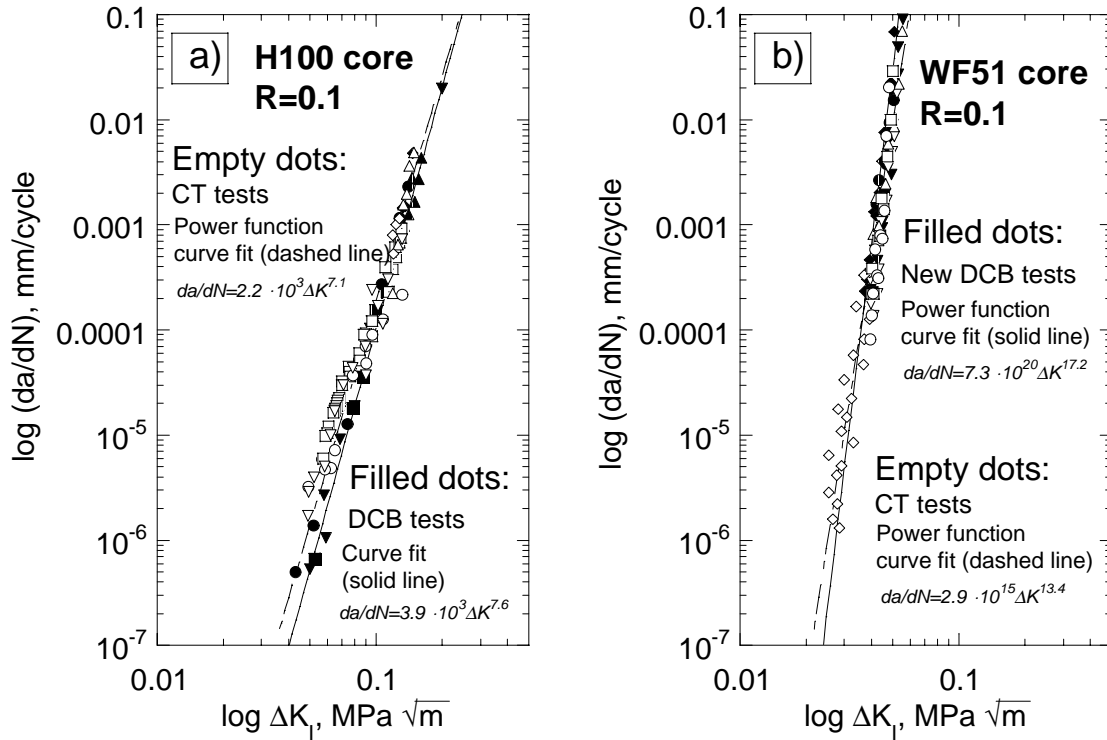


Fig. 4: A comparison of the results from the DCB and the CT testing. Fatigue crack growth rates  $da/dN$  versus stress intensity factor  $\Delta K$  for H100 core (a) and WF51 core (b) tested at  $R=0.1$  and 60% of the static fracture load.

As can be seen in the Fig. 4, fatigue data from different test specimens are in a very good agreement and quite consistent with each other for both core materials. This undoubtedly encourages the reliability of the obtained FCG rates and their applicability for further analysis. A more detailed discussion is provided below.

#### Comparison of the FCG rates for the H100 and the WF51 cores

Quantitative comparison of the derived Paris' law equations, given in the Fig. 4(a,b), reveals that the values of the coefficients  $C$  and  $m$ , which characterize the rates of the fatigue crack propagation, are significantly higher for the WF51 core than for the H100 core. This was believed to be due to the higher brittleness and lower density of the WF51 core material.

#### Influence of the face/core interface on FCG rates

Although, the fatigue data for the DCB and the CT specimens appeared to coincide with each other, a slightly higher values of the coefficient  $m$  in the derived Paris' law equations for the DCB specimens can indicate to the faster FCG rates in the face/core interface region. It was observed for the both considered core materials. It may be assumed to be due to the influence of the face/core interface with different mechanical properties. However, this hypothesis has to be further investigated.

### *Fatigue threshold characterization*

The low FCG rates only down to  $10^{-6}$  mm/cycle were achieved in the DCB and the CT specimens, tested under a  $K$ -decreasing technique. At these FCG rates no crack retardation was noticed, which usually indicates the approach of stress intensity threshold values  $\Delta K_{th}$ . It is practically troublesome to achieve lower FCG rates because of the above mentioned problem with the discrete crack extension, if considered on the microscale level, when the cell size is comparable with such low fatigue crack extensions. Moreover, such tests are quite time consuming at test frequency of 2 Hz. ASTM Standard E647-95a [11] and proposed by Bucci standard for near-threshold FCG rate measurements [14] suggest to define stress intensity threshold values  $\Delta K_{th}$  at the FCG rates of  $10^{-8}$  mm/cycle.

For the DCB and the CT specimens, stress intensity threshold values  $\Delta K_{th}$  were derived by extrapolating power function curve fits down to the required FCG rates of  $10^{-8}$  mm/cycle. Linear slope of the experimental data was assumed. Threshold stress intensity values  $\Delta K_{th}$  are given in Table 2. They were found to be in a good agreement with each other and roughly their values are 20% of the fracture toughness values.

## **CONCLUSIONS**

From the analysis of the presented results the following conclusions can be made:

- Results from the DCB and the CT specimens were in a good agreement with each other, encouraging the reliability of measured FCG rates and their applicability for the further analysis.
- Fatigue crack growth data for the considered cellular foams may be analyzed in terms of the classical Paris' law as for conventional metallic materials. The experimental data did not reveal a crack retardation in the region of low stress intensity factors at the FCG rates down to  $10^{-6}$  mm/cycle.
- FCG rates for the WF51 core were found to be significantly higher in comparison to the H100 core.
- A small influence of the face/core interface in DCB specimens on the FCG rates was revealed from the analysis of derived Paris' relationships for the DCB and the CT experiments. The FCG rates in the face/core interface appeared to be slightly faster in comparison to the crack propagation rates in the virgin core material.

## **REFERENCES**

1. Gibson, L.J. and Ashby, M.F., *Cellular Solids - Structures and Properties*, Pergamon, Oxford, 1988.
2. Zenkert, D. and Bäcklund, J., "PVC Sandwich Core Materials: Mode I Fracture Toughness", *Composites Science and Technology*, Vol. 34, 1989, pp. 225-242.

3. Zenkert, D., "PVC Sandwich Core Materials: Fracture Behaviour under Mode II and Mixed Mode Conditions", *Materials Science and Engineering*, Vol. A108, 1989, pp. 233-240.
4. McIntyre, A. and Anderton, G.E., "Fracture Properties of Rigid Polyurethane Foam over a Range of Densities", *Polymers*, Vol. 20, 1979, pp. 247-253.
5. Shipsha, A., Burman, M. and Zenkert, D., "Interfacial Fatigue Crack Growth in Foam Core Sandwich Structures", accepted for publication in *International Journal of Fatigue and Fracture of Engineering Materials and Structures*.
6. Noury, P.M.C., Sheno, R.A. and Sinclair, I., "Fatigue Crack Growth in Rigid PVC Cellular Foam Under Combined Mode I and Mode II Loading", *Proceedings of the Forth International Conference on Sandwich Construction*, Stockholm, Sweden, June 9-11, 1998, Vol. II: Core Materials, Olsson, K.-A., Ed., pp. 491-502.
7. Shipsha, A., Burman, M. and Zenkert, D., "On Mode I Fatigue Crack Growth in Foam Core Materials for Sandwich Structures", to be submitted.
8. Li, X. and Carlsson, L.A., "A Test Specimen for Determining the Fracture Resistance of a Facing/Core Interface", *Proceedings of the Forth International Conference on Sandwich Construction*, Stockholm, Sweden, June 9-11, 1998, Vol. II: Experimental Investigations, Olsson, K.-A., Ed., pp. 647-658.
9. DIVINYCELL, Technical Manual H-grade, Divinycell International AB, Laholm, Sweden, 1995.
10. ROHACELL, Technical Manual, Rohm GmbH, Germany, 1987.
11. ASTM E647-95a, *Standard Test Method for Measurement of Fatigue Crack Growth Rates*, Annual Book of ASTM Standards, Philadelphia, 1995.
12. Blom, A., "An Assessment of Different Experimental Techniques for Determination of the Threshold Stress Intensity Factor  $\Delta K_{th}$ ." Report 82-2, *Department of Aeronautics*, Royal Institute of Technology, Stockholm, Sweden, 1982.
13. Schubert, O., "Fracture Toughness Tests of Sandwich Core Materials." Report 94-3, *Department of Aeronautics*, Royal Institute of Technology, Stockholm, Sweden, 1994.
14. Bucci, R.J., "Development of a Proposed ASTM Standard Test Method for Near-Threshold Fatigue Crack Growth Rate Measurement." *Fatigue Crack Growth Measurement and Data Analysis*, ASTM STP 738, S.J. Hudak, Jr., and R.J. Bucci, Eds., American Society for Testing and Materials, 1981, pp. 5-28.